

SDSS Absolute Magnitudes for Thin Disc Stars based on Trigonometric Parallaxes

S. Bilir,^{1*} S. Karaali², S. Ak¹, K. B. Coşkunoglu¹, E. Yaz¹ A. Cabrera-Lavers^{3,4}

¹*Istanbul University Science Faculty, Department of Astronomy and Space Sciences, 34119, University-Istanbul, Turkey*

²*Beykent University, Faculty of Science and Letters, Department of Mathematics and Computer, Beykent 34398, Istanbul, Turkey*

³*Instituto de Astrofísica de Canarias, E-38205 La Laguna, Tenerife, Spain*

⁴*GTC Project Office, E-38205 La Laguna, Tenerife, Spain*

Accepted 2007 month day. Received year month day;

ABSTRACT

We present a new luminosity-colour relation based on trigonometric parallaxes for thin disc main-sequence stars in SDSS photometry. We matched stars from the newly reduced Hipparcos catalogue with the ones taken from 2MASS All-Sky Catalogue of Point Sources, and applied a series of constraints, i.e. relative parallax errors ($\sigma_\pi/\pi \leq 0.05$), metallicity ($-0.30 \leq [M/H] \leq 0.20$ dex), age ($0 \leq t \leq 10$ Gyr) and surface gravity ($\log g > 4$), and obtained a sample of thin disc main-sequence stars. Then, we used our previous transformation equations (Bilir et al. 2008a) between SDSS and 2MASS photometries and calibrated the M_g absolute magnitudes to the $(g-r)_0$ and $(r-i)_0$ colours. The transformation formulae between 2MASS and SDSS photometries along with the absolute magnitude calibration provide space densities for bright stars which saturate the SDSS magnitudes.

Key words: Galaxy: disc, Galaxy: solar neighbourhood, stars: distances

1 INTRODUCTION

Among several large sky surveys, two have been used most widely in recent years. The first, Sloan Digital Sky Survey (SDSS, York et al. 2000), is the largest photometric and spectroscopic survey in optical wavelengths. The second, Two Micron All Sky Survey (2MASS, Skrutskie et al. 2006) has imaged the sky in infrared. SDSS obtains images almost simultaneously in five broad-bands (u , g , r , i and z) centered at 3540, 4760, 6280, 7690 and 9250 Å, respectively (cf. Fukugita et al. 1996). The photometric pipeline detects the objects, then matches the data from five filters and measures instrumental fluxes, positions and shape parameters. The shape parameters allow the classification of objects as point source or extended. The limiting magnitudes of the passbands are 22, 22.2, 22.2, 21.3, and 20.5 for u , g , r , i , and z , respectively. The data are saturated at about 14 mag in g , r , and i , and about 12 mag in u and z (cf. Chonis & Gaskell 2008).

2MASS provides the most complete database of near-infrared (NIR) galactic point sources. During the development of this survey, two highly automated 1.3m telescopes were used: one at Mt. Hopkins, Arizona to observe the Northern sky, and the other at Cerro Tololo Observatory,

Chile to survey the Southern half. Observations cover 99.998 per cent (Skrutskie et al. 2006) of the sky with simultaneous detections in J (1.25 μm), H (1.65 μm) and K_s (2.17 μm) bands up to limiting magnitudes of 15.8, 15.1 and 14.3, respectively. The passband profiles for $ugriz$ and JHK_s photometric systems are given in Fig. 1 (Bilir et al. 2008a).

Saturation of the $ugriz$ data at bright magnitudes is a disadvantage for galactic surveys. Actually, space densities can not be evaluated for distances less than ~ 0.5 kpc due to this saturation. The number of distance intervals without space densities is even larger for bright absolute magnitude intervals. On the other hand, 2MASS is a shallow survey, i.e. it contains relatively bright point sources, which can be used to fill up the gap of SDSS photometry for short distances. Our aim is to use the transformations between 2MASS and SDSS given in our previous paper (Bilir et al. 2008a) and to calibrate the M_g absolute magnitude using $(g-r)_0$ and $(r-i)_0$ colours based on Hipparcos trigonometric parallaxes. Thus, two sets of data will be used in estimating galactic model parameters: The first set is the JHK_s data of relatively nearby stars in a given field of the Galaxy. The second one consists of SDSS data of stars occupying further distances in the same field. For the first set, 2MASS data needs to be transformed into SDSS data before applying procedures used in estimating absolute magnitude, whereas

* E-mail: sbilir@istanbul.edu.tr

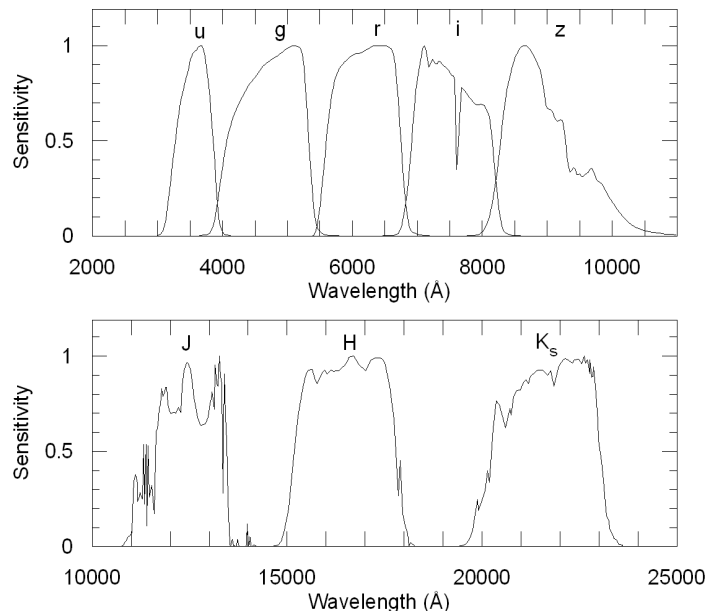


Figure 1. Normalized passbands of SDSS filters (upper panel), and 2MASS filters (lower panel).

for the second set of data (the SDSS data) the procedures can be applied directly.

In Section 2, the data and the determination of the sensitive sample are presented. The procedure and absolute magnitude calibration are given in Section 3 and the results are discussed in Section 4. Finally, a conclusion is given in Section 5.

2 THE DATA

We matched stars from the newly reduced Hipparcos catalogue (van Leeuwen 2007) with the ones from 2MASS All-Sky Catalog of Point Sources (Cutri et al. 2003), and applied a series of constraints in order to obtain a sample of thin disc main-sequence stars. To produce the sample, the first constraint we applied was to choose the 11644 stars from the newly reduced Hipparcos catalogue (van Leeuwen 2007) with relative parallax errors $\sigma_\pi/\pi \leq 0.05$. Then, we omitted the stars without 2MASS data. Afterwards, to eliminate reddening, 2MASS magnitudes were de-reddened using the procedure given by Bilir et al. (2008a), even though the program stars are relatively close and the near-infrared reddening correction is very small. The second restriction was to limit the absolute magnitude between $0 < M_J < 6$, which corresponds to the spectral type range A0–M0. The estimation of the absolute magnitude range can be seen from the 2MASS colour-magnitude diagram (Fig. 2). Finally, we adopted the procedure used in our previous paper (Bilir et al. 2008b) to exclude evolved, thick disc and halo stars from the sample. The mentioned procedure requires the following limitations for metallicity, age and surface gravity taken from Padova isochrones (Marigo et al. 2008): $-0.30 \leq [M/H] \leq 0.20$ dex, $0 \leq t \leq 10$ Gyr and $\log g > 4$, respectively. Thus, to establish the luminosity–colour relation, we produced a thin disc sample of 4449 main-sequence stars with accurate trigonometric parallaxes

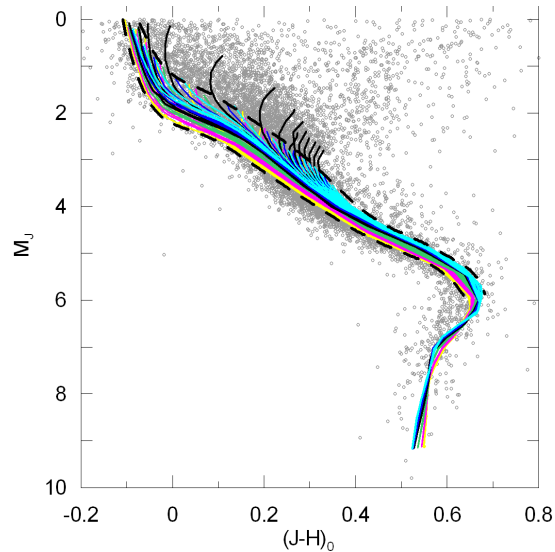


Figure 2. $M_J/(J-H)_0$ colour-absolute magnitude diagram for the original sample. The upper and lower envelopes (the dashed lines) show the final sample, i.e. thin disc main-sequence stars. The thin curves correspond to Padova isochrones.

and 2MASS data. The typical near-infrared colour and absolute magnitude errors of our sample are ± 0.04 and ± 0.14 mag, respectively. Lutz & Kelker (1973) stated that there is a systematic error in computed distances, which only depends on the σ_π/π ratio. Jerzykiewicz (2001) showed that the error is negligible if $\sigma_\pi/\pi \leq 0.10$, which is the case in this study as $\sigma_\pi/\pi \leq 0.05$.

3 THE PROCEDURE AND ABSOLUTE MAGNITUDE CALIBRATION

We adopted the metallicity sensitive Eqs. (13), (18), and (19) from Bilir et al. (2008a) for the calibration of M_g absolute magnitudes for our star sample. These equations are as follows:

$$(g-r)_0 = 1.361(\pm 0.016)(g-r)_0 + 1.724(\pm 0.019)(r-i)_0 + 0.521(\pm 0.009), \quad (1)$$

$$(g-r)_0 = 1.991(\pm 0.040)(J-H)_0 + 1.348(\pm 0.066)(H-K_s)_0 - 0.247(\pm 0.019), \quad (2)$$

$$(r-i)_0 = 1.000(\pm 0.036)(J-H)_0 + 1.004(\pm 0.064)(H-K_s)_0 - 0.220(\pm 0.017). \quad (3)$$

We transformed $(J-H)_0$ and $(H-K_s)_0$ colours of the stars in our sample into $(g-r)_0$ and $(r-i)_0$ colours using Eqs. (2) and (3). Then, we used these colours and the J_0 magnitudes in Eq. (1) and obtained the g_0 magnitudes for the star sample. Finally, combining the g_0 magnitudes and Hipparcos parallaxes of stars we obtained accurate M_g absolute magnitudes.

Now, we have two sets of SDSS data, i.e. M_g absolute magnitudes and $(g-r)_0$ and $(r-i)_0$ colours for 4449 thin

disc main-sequence stars. We can adopt a procedure similar to the one used in our recent works (Bilir et al. 2005, 2008b) and calibrate the M_g absolute magnitude to SDSS colours $(g-r)_0$ and $(r-i)_0$ as follows:

$$M_g = a_1(g-r)_0^2 + b_1(r-i)_0^2 + c_1(g-r)_0(r-i)_0 + d_1(g-r)_0 + e_1(r-i)_0 + f_1. \quad (4)$$

We applied the covariance matrices of the solutions (1), (2) and (3) and obtained the individual estimation errors depending on the actual coefficients. These errors are given in the parentheses in Eqs. (1), (2) and (3) correspond to the dispersion of the observations. If we assume a total noise of approximately 0.1 associated with these calibrations, the complement error can be attributed to cosmic noise.

The numerical values of the coefficients in Eq. (4) and their errors, the corresponding standard deviation and the squared correlation coefficient are given in Table 1. One can deduce that the error in absolute magnitude M_g is of order 0.19 (the standard deviation). This is true when the colours in Eq. (4) are free of errors. However, this is not the case. The colours are associated with the errors given for the Eqs. (1), (2) and (3). Hence, one expects an additional error originating from the colours. We added the errors of the colours $(g-r)_0$ and $(r-i)_0$ to their observed values and reevaluated the absolute magnitudes by Eq. (4). For simplicity, we called absolute magnitudes evaluated using this procedure M'_g . As expected, there is a mean offset of 0.12 mag from the Hipparcos absolute magnitudes. The standard deviation of $\Delta M_g = (M_g)_{Hip} - M'_g$ is 0.19. Hence, the total and maximum error for the absolute magnitude evaluated by Eq. (4) is $\sqrt{2} \times 0.19 = 0.27$ mag.

3.1 Testing the procedure

We tested our procedure by comparing the M_g absolute magnitudes calculated by means of Eq. (4) with the ones evaluated via combining g_0 apparent magnitudes and trigonometric parallaxes adopted from the newly reduced Hipparcos catalogue (van Leeuwen 2007). Fig. 3 shows that there is a one-to-one correspondence between two sets of M_g absolute magnitudes. Also, the mean and the standard deviation of differences inbetween original absolute magnitudes and calculated absolute magnitudes are rather small, i.e. $\langle \Delta M_g \rangle \approx 0.00$ and $s = 0.19$ mag.

Most of the sample stars were obtained by applying a series of constraints to the newly reduced Hipparcos catalogue. These stars lie within 2σ (upper panel in Fig. 3). However, the $\Delta M_g = (M_g)_{Hip} - (M_g)_c$ residuals give the impression of a small, but systematic drift. That is, the calculated absolute magnitudes are a bit larger than the expected ones for faint absolute magnitudes. Keeping in mind the data sample were reduced from 11644 (original sample) to 4449, one can try to explain this drift with applied constraints. We should add that our aim in this work is to obtain absolute magnitudes for a pure thin disc population, so applying the constraints was needed. Hence, the results of the applied constraints are unavoidable.

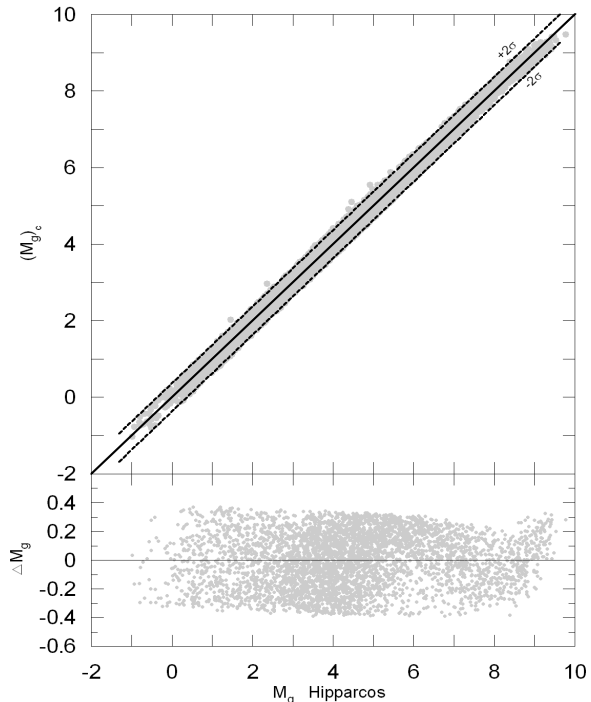


Figure 3. $(M_g)_c$ absolute magnitudes estimated using Eq. (4) versus M_g absolute magnitudes calculated from newly reduced Hipparcos data (upper panel) and variation of the differences between two sets of absolute magnitudes (lower panel). All calibration stars in the figure are located within the prediction limit of 2σ .

3.2 Comparison of absolute magnitudes using different datasets

We compared the M_g absolute magnitudes determined in this work with the ones appearing in the literature. Comparison with the data of Covey et al. (2007) and SEGUE data of SDSS DR6 by means of Allende Prieto et al.'s (2006) method could be carried out after some reductions and/or constraints, whereas a direct comparison could be made with Karaali et al. (2005), Bilir et al. (2005), Jurić et al. (2008) and Just & Jahreiss (2008).

3.2.1 Comparison with the data of Covey et al. (2007)

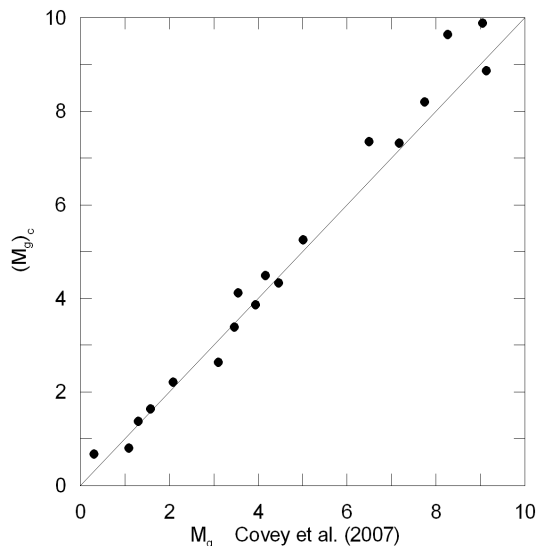
Covey et al. (2007) used the synthetic library of Pickles (1998) and evaluated the M_J absolute magnitudes and, $(g-r)_0$ and $(r-i)_0$ colours for 18 main-sequence stars of different spectral types (Table 2). Using these values in the following equation (Eq. 5), modified from Eq. (1), we obtained the corresponding M_g absolute magnitudes. Then, we compared these values with $(M_g)_c$ absolute magnitudes, which were calculated using Eq. (4).

$$M_g - M_J = 1.361(\pm 0.016)(g-r)_0 + 1.724(\pm 0.019)(r-i)_0 + 0.521(\pm 0.009). \quad (5)$$

There is an agreement between the two sets of absolute magnitudes (Table 2 and Fig. 4) confirming our new procedure for absolute magnitude determination. The small drift in the vertical direction in Fig. 4 for the faint absolute magnitudes originates from the application of two different procedures.

Table 1. Coefficients and their standard errors for Eq. (4). R^2 and s denotes the squared correlation coefficient and the standard deviation, respectively.

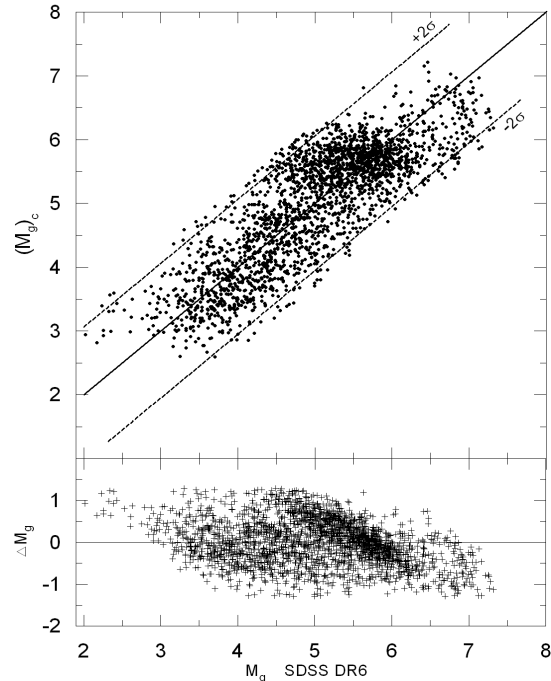
a_1	b_1	c_1	d_1	e_1	f_1	R^2	s
-0.719 (± 0.186)	1.953 (± 0.681)	-0.474 (± 0.072)	10.697 (± 0.196)	-9.350 (± 0.306)	1.668 (± 0.027)	0.99	0.19

**Figure 4.** $(M_g)_c$ absolute magnitudes estimated using Eq. (4) versus M_g absolute magnitudes calculated from Covey et al.'s data (2007).

Although all the data, i.e. M_J , $(g-r)_0$ and $(r-i)_0$, were taken from Covey et al. (2007), the $(M_g)_c$ absolute magnitudes (on the Y-axis) were evaluated only using $(g-r)_0$ and $(r-i)_0$ colours and Eq. (4), whereas M_g absolute magnitudes (on the X-axis) were evaluated by substituting these colours and M_J absolute magnitudes in Eq. (5).

3.2.2 Comparison with SDSS DR6

The second dataset we compared ours to is the Sloan Extension for Galactic Understanding and Exploration (SEGUE) data of SDSS Data Release 6 (DR6). Spectra for over 250000 stars in the galactic disc and spheroid for all common spectral types exist in SEGUE¹. These spectra were processed with a pipeline called the ‘‘Spectro Parameter Pipeline’’ (spp) which computes standard stellar atmospheric parameters such as $[Fe/H]$, $\log g$ and T_{eff} for each star by a variety of methods. We used the parameters evaluated by Allende Prieto et al.'s (2006) model-atmosphere analysis method and applied the following constraints in order to obtain a thin disc sample: $4 \leq \log g \leq 4.5$ and $-0.3 \leq [M/H] \leq +0.2$ dex. The M_g absolute magnitudes of 2289 stars, which satisfied our constraints, were evaluated by combining their g_0 apparent magnitudes and distances. The comparison of these absolute magnitudes with the ones determined using Eq. (4), $(M_g)_c$, is shown in Fig. 5. There is an agreement between the two sets of absolute magnitudes. However, the dispersion is larger than the ones in Figs. 3 and 4. Also, there

**Figure 5.** $(M_g)_c$ absolute magnitudes estimated using Eq. (4) versus M_g absolute magnitudes calculated from SEGUE data of SDSS DR6 by means of Allende Prieto et al.'s (2006) method (upper panel) and variation of the differences between two sets of absolute magnitudes (lower panel). The dashed lines denote the 2σ prediction limits.

are clearly visible systematic effects shown in the distributions, in particular at $(M_g)_c = 6$. These effects probably originate from a series of constraints applied to the data, i.e. 1) we used the atmospheric parameters evaluated using Allende Prieto et al.'s (2006) method, 2) we selected stars with $4 \leq \log g \leq 4.5$, and 3) we limited the metallicities with $-0.3 \leq [M/H] \leq +0.2$ dex in order to obtain a pure thin disc population. It seems that all these limitations caused the systematic effects mentioned above.

3.2.3 Comparison with data appearing in the literature

Karaali et al. (2005) used observations obtained in $u'g'r'$ filters at Isaac Newton Telescope (INT) at La Palma in Spain. The filters were designed to reproduce the SDSS system. The data was complemented by Landolt (1992) UBV standard star photometry and was used to calculate transformations between the INT SDSS $u'g'r'$ filter-detector combination and standard Johnson-Cousins photometry. Karaali et al. (2005) presented transformation equations depending on two colours for the first time. The M_g absolute magnitudes evaluated by these equations agree with the $(M_g)_c$ absolute magnitudes calculated using Eq. (4) in this work (Fig. 6).

¹ <http://cas.sdss.org/seguedr6/en/tools/search/sql.asp>

Table 2. Comparison of the absolute magnitudes calculated in our work with the absolute magnitudes of Covey et al. (2007). Data in columns (1-4) were taken from Covey et al. (2007). $(M_g)_c$ is calculated using Eq. (4) and the data in columns (3-4), M_g is the absolute magnitude evaluated using Bilir et al.'s (2008a) procedure and the data in columns (2-4). ΔM_g is the difference between M_g and $(M_g)_c$.

Spectral Type	M_J	$(g-r)_0$	$(r-i)_0$	M_g	$(M_g)_c$	ΔM_g
A0V	0.430	-0.250	-0.180	0.300	0.674	-0.374
A2V	1.170	-0.230	-0.170	1.085	0.797	0.288
A3V	1.250	-0.160	-0.150	1.295	1.373	-0.078
A5V	1.380	-0.100	-0.110	1.575	1.638	-0.063
A7V	1.730	-0.020	-0.080	2.086	2.214	-0.128
F0V	2.430	0.100	0.010	3.104	2.637	0.467
F2V	2.630	0.190	0.030	3.461	3.393	0.068
F5V	2.620	0.260	0.030	3.547	4.118	-0.571
F6V	2.900	0.280	0.080	3.940	3.861	0.079
F8V	2.980	0.360	0.100	4.163	4.493	-0.330
G0V	3.180	0.380	0.140	4.460	4.333	0.127
G5V	3.540	0.490	0.160	5.004	5.254	-0.250
K2V	4.500	0.780	0.240	6.496	7.354	-0.858
K3V	4.940	0.850	0.320	7.170	7.320	-0.150
K4V	5.210	1.000	0.380	7.747	8.195	-0.448
K5V	5.450	1.180	0.400	8.267	9.638	-1.371
K7V	5.770	1.340	0.540	9.046	9.888	-0.842
M0V	5.720	1.310	0.640	9.127	8.866	0.261

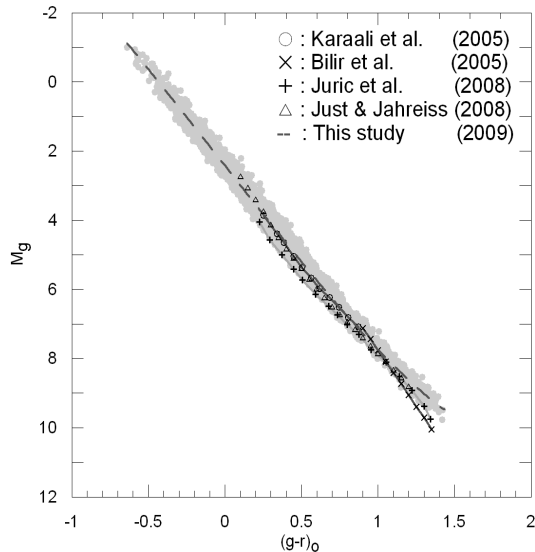


Figure 6. $M_g/(g-r)_0$ colour-magnitude diagram for different studies.

The best fit in Fig. 6 is between the colour-absolute magnitude diagrams obtained in our work and in the work of Karaali et al. (2005). Actually, the open circle symbols used for the data of Karaali et al. (2005) and the locus of the grey circles representing the data in this work overlap.

The transformations between SDSS and UBVRI photometries in our previous work (Bilir et al. 2005) provides M_g absolute magnitudes for late-type dwarfs. We compared the $(M_g)_c$ absolute magnitudes determined using Eq. (4) and the ones obtained using the procedure in Bilir et al. (2005) to notice any possible deviation. Fig. 6 shows that the agreement is limited with colours $(g-r)_0 < 1.2$ mag.

Just & Jahreiss (2008) applied the transformation equations of Chonis & Gaskell (2008) to the 786 star sample in the solar neighbourhood ($r \leq 25$ pc) and obtained a mean

$M_g/(g-r)_0$ main sequence in 0.05 mag bins. The nearby stars represent the thin disc population completely. Hence, we expect an agreement between the M_g absolute magnitudes evaluated in our work and in Just & Jahreiss (2008). Fig. 6 shows that this is the case.

The only deviation is noticed between our M_g absolute magnitudes and those of Jurić et al. (2008) (Fig. 6). However, their $M_g/(g-r)_0$ colour-magnitude diagram is a combination of apparent colour-magnitude diagrams and that may be the reason of the deviation mentioned (see Discussion).

3.3 Alternative procedure

We applied an alternative procedure to our sample of 4449 thin disc main-sequence stars to evaluate the M_g absolute magnitudes, explained as follows. First, we transformed their $(J-H)_0$ and $(H-K_s)_0$ colours into $(g-r)_0$ and $(r-i)_0$ colours using Eqs. (2) and (3). Then, we used these colours and the corresponding M_J absolute magnitudes, evaluated by the luminosity-colour relations of Bilir et al. (2008b), in Eq. (5) and obtained the M_g absolute magnitudes of the sample stars. We compared the M_g absolute magnitudes evaluated by this procedure with the ones determined by the combining their apparent g_0 magnitudes and trigonometric parallaxes taken from the newly reduced Hipparcos catalogue (van Leeuwen 2007). Fig. 7 confirms the agreement between the two sets of M_g absolute magnitudes. From the comparison of Fig. 3 and Fig. 7, one can deduce that the alternative procedure favours the procedure explained in Section 3. That is, the combination of $(g-r)_0$ and $(r-i)_0$ and M_J absolute magnitude supplies more accurate M_g absolute magnitudes by means of Eq. (5) than the combination of the same colours alone in Eq. (4). Actually, the mean of the offsets and the corresponding standard deviations for the data in Fig. 7 are $\Delta M_g = 0.00$ and $s = 0.03$, respectively, whereas they are $\Delta M_g \cong 0.00$ and $s = 0.19$ for the data in

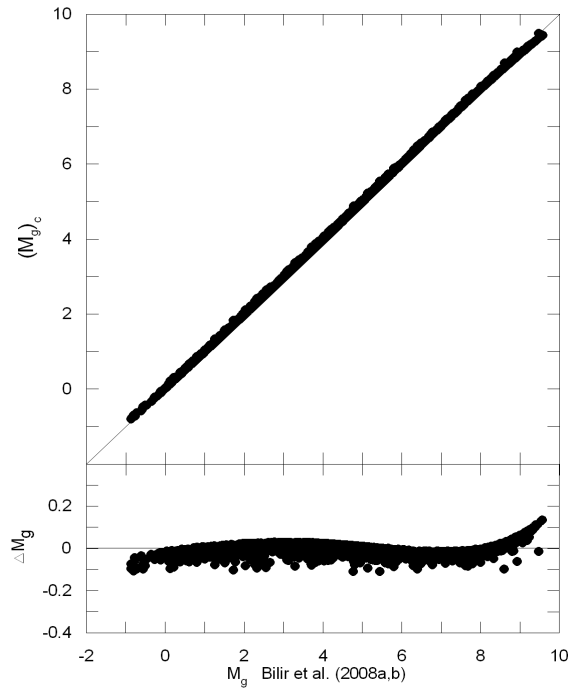


Figure 7. M_g absolute magnitudes estimated using Eq. (5) versus $(M_g)_c$ absolute magnitudes calculated from newly reduced Hipparcos data (upper panel) and variation of the differences between two sets of absolute magnitudes (lower panel).

Fig. 3. The sharp limits of the residuals in the lower panel in Fig. 7 are due to concentration of the residuals with small standard deviation. We confess that, in order to obtain this figure, we omitted 36 sample stars with $\Delta M_g < -0.10$ mag which are not of 'AAA' quality flag.

3.4 Binarism Effect

A high fraction of stars are in fact binary systems and being a binary system makes stars appear brighter and redder than they normally are. Different fractional values (defined as f) can be found in the literature. As it was quoted in our previous work (Bilir et al. 2008b, and the references therein), the range of f is $0.4 \leq f < 1$. Kroupa, Gilmore & Tout (1991) found that for the extreme value, i.e. $f = 1$, a single mass function provides the best representation of a single luminosity function.

In our previous work (Bilir et al. 2008b) we adopted a simple but reasonable procedure and revealed the binarism effect for M_V and M_J absolute magnitudes. The scatter in absolute magnitude as a function of binary fraction f was found to be $\Delta M_J = 0.266 \times f + 0.014$. In this work, the calibration of M_g absolute magnitudes to $(g-r)_0$ and $(r-i)_0$ colours is carried out using the 2MASS data. Hence, we can adopt the same calibration for the scatter in M_g , i.e.

$$\Delta M_g = 0.266 \times f + 0.014. \quad (6)$$

4 DISCUSSION

We matched stars taken from the newly reduced Hipparcos catalogue (van Leeuwen 2007) with the ones taken from

2MASS All-Sky Catalogue of Point Sources (Cutri et al. 2003), and applied a series of constraints in order to obtain a sample of thin disc main-sequence stars. These constraints reduced the original sample of 11644 stars with relative parallax errors $\sigma_\pi/\pi \leq 0.05$ to 4449. Then, we used the 2MASS data in the transformation equations presented in our previous work (Bilir et al. 2008a) and calibrated the M_g absolute magnitudes to the SDSS colours, i.e. $(g-r)_0$ and $(r-i)_0$.

The advantage of this procedure is that it uses a specific sample of nearby stars with small parallax errors. The constraints, i.e. $-0.30 \leq [M/H] \leq 0.20$ dex, $0 \leq t \leq 10$ Gyr and $\log g > 4$, exclude any contamination of evolved thin and thick disc stars and halo stars. Thus, we obtained a colour-magnitude diagram which provides accurate M_g absolute magnitudes for the thin disc main-sequence stars. The calibration can be used directly for faint stars, whereas for bright stars with saturated SDSS magnitudes one needs to transform the 2MASS data into SDSS data via our previous transformation formulae (Bilir et al. 2008a).

We compared the $M_g/(g-r)_0$ colour-magnitude diagram obtained in this study with six others appearing in the literature. The best fit is between our diagram and that of Karaali et al. (2005) which indicates that there are no systematic deviations between the in $u'g'r'$ filters at INT and the original SDSS filters.

Since Just & Jahreiss (2008) used a sample of 786 stars in the solar neighbourhood, which have a much higher probability of consisting of pure thin disc main-sequence stars, their results are precise. The precision of Just & Jahreiss' (2008) results along with the agreement level between our data and theirs confirms our calibration.

The M_g absolute magnitudes evaluated from the synthetic data of Covey et al. (2007) also agree with our M_g absolute magnitudes. The same agreement holds for the M_g absolute magnitudes of SEGUE data of SDSS DR6 by means of Allende Prieto et al.'s (2006) method, however, with larger dispersion.

$M_g/(g-r)_0$ colour-magnitude diagram of Jurić et al. (2008) deviates from our colour-magnitude diagram and from those cited above. These authors compared the $M_g/(g-r)_0$ colour-magnitude diagrams appearing in the literature and used two colour-magnitude diagrams, one for bright stars and one for faint stars in their extensive work. We preferred the one for bright stars in this comparison due to our sample of stars being bright. However, we could not avoid the deviation mentioned.

Finally, we should note that the $M_g/(g-r)_0$ colour-magnitude diagram presented in this work agrees with the previous one (Bilir et al. 2005) for stars with $(g-r)_0 < 1.2$ mag, but there is a deviation for red stars which increases slightly with $(g-r)_0$ colour.

5 CONCLUSION

We calibrated the M_g absolute magnitudes to the $(g-r)_0$ and $(r-i)_0$ colours by using the newly reduced Hipparcos catalogue and 2MASS data for thin-disc main-sequence stars with bright apparent magnitude which can be used in evaluating space densities for nearby stars. Thus, any possible degeneration due to extrapolation of density functions

to zero distance should be avoided. This will lead to more accurate galactic model parameter estimation.

6 ACKNOWLEDGMENTS

We would like to thank the referee Floor van Leeuwen for his suggestions towards improving the paper. Also, we would like to thank Dr. Martin López-Corredoira for his valuable contributions. S. Karaali is grateful to the Beykent University for financial support.

REFERENCES

- Allende Prieto C., Beers T. C., Wilhelm R., Newberg H. J., Rockosi C. M., Yanny B., Lee Y. S., 2006, *ApJ*, 636, 804
- Bilir S., Karaali S., Tunçel, S., 2005, *AN*, 326, 321
- Bilir S., Ak S., Karaali S., Cabrera-Lavers A., Chonis T. S., Gaskell C. M., 2008a, *MNRAS*, 384, 1178
- Bilir S., Karaali S., Ak S., Yaz E., Cabrera-Lavers A., Coşkunoglu K. B., 2008b, *MNRAS*, 390, 1569
- Covey K. R., et al., 2007, *AJ*, 134, 2398
- Chonis T. S., Gaskell C. M., 2008, *AJ*, 135, 264
- Cutri R. M., et al., 2003, *2MASS All-Sky Catalogue of Point Sources*, CDS/ADC Electronic Catalogues, 2246
- Fukugita M., Ichikawa T., Gunn J. E., Doi M., Shimasaku K., Schneider D. P., 1996, *AJ*, 111, 1748
- Jerzykiewicz M., 2001, *AcA*, 51, 151
- Jurić M., et al., 2008, *ApJ*, 673, 864
- Just A., Jahreiss H., 2008, *AN*, 329, 790
- Karaali S., Bilir S., Tunçel S., 2005, *PASA*, 22, 24
- Kroupa P., Gilmore G., Tout C. A., 1991, *MNRAS*, 251, 293
- Landolt A. U., 1992, *AJ*, 104, 340
- Lutz T. E., Kelker D. H., 1973, *PASP*, 85, 573
- Marigo P., Girardi L., Bressan A., Groenewegen M. A. T., Silva L., Granato G. L., 2008, *A&A*, 482, 883
- Pickles A. J., 1998, *PASP*, 110, 863
- Skrutskie M. F., et al., 2006, *AJ*, 131, 1163
- York D. G., et al., 2000, *AJ*, 120, 1579
- van Leeuwen F., 2007, *A&A*, 474, 653